Validation of leading point concept in RANS simulations of highly turbulent lean syngas-air flames with well-pronounced diffusional-thermal effects

(article starts on next page)

Validation of leading point concept in RANS simulations of highly turbulent lean syngas-air flames with well-pronounced diffusional-thermal effects
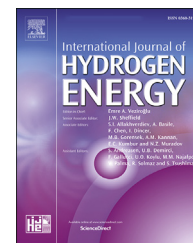
Salman Verma [a,b], Florian Monnier [c], Andrei N. Lipatnikov [d,*]

[a] Department of Mechanical Engineering, University of Maryland, College Park, MD 20742, USA
[b] John Zink Company, LLC, Tulsa, OK 74116, USA
[c] CORIA - CNRS, Normandie Université, INSA de Rouen Normandie, 76000 Rouen, France
[d] Department of Mechanics and Maritime Sciences, Chalmers University of Technology, Gothenburg, 41296 Sweden

HIGHLIGHTS

- Leading point concept is adapted for CFD research into complex-chemistry flames.
- Atlanta experiments with highly turbulent lean syngas-air mixtures are simulated.
- An increase in turbulent burning velocity with increasing H_2/CO ratio is predicted.

ARTICLE INFO

ABSTRACT

While significant increase in turbulent burning rate in lean premixed flames of hydrogen or hydrogen-containing fuel blends is well documented in various experiments and can be explained by highlighting local diffusional-thermal effects, capabilities of the vast majority of available models of turbulent combustion for predicting this increase have not yet been documented in numerical simulations. To fill this knowledge gap, a well-validated Turbulent Flame Closure (TFC) model of the influence of turbulence on premixed combustion, which, however, does not address the diffusional-thermal effects, is combined with the leading point concept, which highlights strongly perturbed leading flame kernels whose local structure and burning rate are significantly affected by the diffusional-thermal effects. More specifically, within the framework of the leading point concept, local consumption velocity is computed in extremely strained laminar flames by adopting detailed combustion chemistry and, subsequently, the computed velocity is used as an input parameter of the TFC model. The combined model is tested in RANS simulations of highly turbulent, lean syngas-air flames that were experimentally investigated at Georgia Tech. The tests are performed for four different values of the inlet rms turbulent velocities, different turbulence length scales, normal and elevated (up to 10 atm) pressures, various H_2/CO ratios ranging from 30/70 to 90/10, and various equivalence ratios ranging from 0.40 to 0.80. All in all, the performed 33 tests indicate that the studied combination of the leading point concept and the TFC model can predict well-pronounced diffusional-thermal effects in lean highly turbulent syngas-air flames, with these results being obtained using the same value of a single constant of the combined model in all cases. In particular, the

model well predicts a significant increase in the bulk turbulent consumption velocity when increasing the H_2/CO ratio but retaining the same value of the laminar flame speed.

Introduction

Due to unique characteristics of H_2-air flames, such as a high laminar burning velocity, a wide range of flammability limits, a low ignition energy, etc. [1], hydrogen is considered to be an additive capable for significantly improving basic characteristics of combustion of fossil fuels [2–10], as well as renewable fuels such as biogas [11–13]. Moreover, renewable synthesis gas (syngas) fuels are primarily composed of H_2 and CO [14]. Accordingly, combustion of fuel blends that contain H_2 is a promising and rapidly developed technology for clean and efficient conversion of energy in stationary power plants, vehicles, and aircrafts. These recent developments have been motivating fundamental research into basic characteristics of laminar [15–17] and turbulent [18–25] burning of fuel blends that contain H_2.

From the fundamental perspective, the most challenging peculiarity of turbulent combustion of lean mixtures that contain H_2 in unburned reactants consists of a significant increase in the burning rates of such mixtures when compared to near-stoichiometric hydrocarbon-air mixtures with similar other characteristics. A number of earlier experimental data that clearly showed this important and well-pronounced phenomenon for lean H_2-air mixtures was reviewed by Lipatnikov and Chomiak [26]. Subsequently, more experimental data of that kind were published, with an extremely strong magnitude of the discussed effect being recently documented by Yang et al. [27]. Such an effect was also measured in lean syngas-air turbulent flames [28–32]. While the effect is less pronounced in fuel blends when compared to pure H_2, the effect magnitude is large even in the former case. It is also worth stressing, that such effects are well documented in experiments not only with weakly turbulent, but also with highly turbulent premixed flames [26,27,30,31].

From the qualitative perspective, the discussed peculiarity of turbulent combustion of lean mixtures that contain H_2 is commonly attributed to diffusional-thermal effects [33–35]. More specifically, if (i) molecular diffusivities of fuel, oxidant, and heat are different and (ii) a flame is perturbed, e.g. curved or/and strained by the flow, then, the local equivalence ratio or/and enthalpy can be increased or decreased within the reaction zone due to imbalance of heat and reactant fluxes from and to the zone, respectively. In a laminar flow, such effects are well-known to cause diffusional-thermal instability of the flame [33]. In a turbulent flow, the diffusional-thermal effects are more pronounced and complicated, e.g. cf. Fig. 6a and b in Ref. [36]. While molecular diffusivities are much smaller than turbulent diffusivities, diffusional-thermal effects can play an important role in turbulent flames, because local gradients of temperature or species concentrations can be high within reaction zones, thus, yielding molecular heat or species fluxes comparable with (or even larger than) the local turbulent fluxes.

The focus of theoretical research into the diffusional-thermal effects is placed on single-step chemistry laminar flames with asymptotically high activation energy [37,38], with differences between molecular transport coefficients being characterized with a single Lewis number $Le = a/\mathcal{D}$. Here, a is the molecular heat diffusivity of the mixture and $\mathcal{D}$ is the molecular diffusivity of the deficient reactant (e.g., fuel in the lean case) in the mixture. Such theories yield analytical expressions for various Markstein numbers [39] $Ma = \delta_L^{-1}(dS_d/d\dot{s})_{\tau_c\dot{s}\to 0}$, which characterize sensitivity of various displacement speeds S_d to the local rate $\dot{s}$ of the flame stretch caused by the flow. Here, $\tau_c = \delta_L/S_L$, δ_L, and S_L are the time scale, thickness, and speed, respectively, of the unperturbed laminar flame (i.e., one-dimensional and planar flame that is stationary in the coordinate framework attached to it) and S_d is the speed of an iso-scalar surface within the flame with respect to the incoming flow of unburned reactants. Note that, in a perturbed flame, not only values of ρS_d are different for different iso-scalar surfaces, but even the signs of the term $(\rho S_d - \rho_u S_L)$ can be different [39,40].

While available theoretical expressions for Ma can easily be used to analyze experimental data or to develop numerical models of turbulent flames [41], such an approach does not seem to be capable for predicting the abnormal increase in turbulent burning rate in lean hydrogen mixtures for a number of reasons discussed elsewhere [26,35,40]. In particular, a theory that addresses a limit of **weak** perturbations ($\tau_c\dot{s}\ll 1$) does not seem to be appropriate for predicting **strong** variations in turbulent burning rate [35]. Accordingly, the present authors are not aware on a simulation that shows ability of a numerical model that describes the diffusional-thermal effects solely by invoking Ma to predict abnormally high turbulent burning rates well documented in lean hydrogen mixtures [26,27].

The present authors are aware on the sole successful attempt [42] to predict this strong effect in a numerical study. In the cited paper, Reynolds-Averaged Navier-Stokes (RANS) simulations of statistically spherical turbulent flames expanding in very lean hydrogen mixtures were performed and abnormally high burning velocities were computed, in quantitative agreement with experiments by Karpov and Severin [43]. The strong increase in turbulent burning velocity was predicted thanks to the use of the so-called leading point concept developed by the Russian school [33,34].

Within the framework of the concept [33–35], propagation of a premixed turbulent flame is hypothesized to be controlled by the leading flame kernels (leading points) that advance

furthest into fresh reactants. Moreover, the structure of such leading flame kernels is hypothesized to be extremely perturbed so that a further increase in the perturbation magnitude would quench combustion locally. Accordingly, turbulent burning velocity is hypothesized to be controlled by the local characteristics of strongly perturbed laminar flame kernels, rather than by characteristics of the unperturbed laminar flame. To use the concept in Computational Fluid Dynamics (CFD) research into turbulent combustion, (i) a model of the leading-flame-kernel structure should be selected and (ii) the kernel characteristics should be pre-computed, followed by (iii) substitution of characteristics of the unperturbed laminar flame, which are commonly used as input parameters when simulating turbulent combustion [44—47], with the counterpart pre-computed characteristics of the leading flame kernel. Since the latter flame kernel is highly perturbed, its characteristics can be very different form characteristics of the unperturbed laminar flame, e.g. the local burning rate can be much higher in lean hydrogen-air mixtures [42]. Therefore, the leading point concept offers an opportunity to predict the strong increase in turbulent burning rate in such mixtures. For this purpose, two different models of the extremely perturbed flame kernels have been suggested: (i) a critically strained laminar flame [34] or (ii) a critically curved laminar flame [48], associated with a flame ball [33]. Characteristics of various critically perturbed laminar flames were compared by Lipatnikov and Chomiak [49].

The leading point concept was supported in recent theoretical [50—52] and Direct Numerical Simulation (DNS) [53—55] studies. Moreover, Venkateswaran et al. [30,31] and Zhang et al. [32] reported that the use of the concept allowed them to significantly improve parameterization of their experimental databases on turbulent burning velocities, obtained from lean syngas-air flames. Nevertheless, the present authors are not aware on the use of the concept in CFD research into turbulent flames, with the exception of a single work [42]. However, in that paper, fuel blends were not considered, and combustion chemistry was reduced to a single reaction. Accordingly, there is a need for assessment of the leading point concept in CFD research into turbulent combustion of fuel blends by allowing for complex combustion chemistry. The present paper aims at filling this knowledge gap by performing RANS simulations of recent experiments done by Venkateswaran et al. [30,31] with highly turbulent lean syngas-air flames.

In the next section, the selected model of leading flame kernels is described, and their characteristics computed using a detailed chemical mechanism are reported. In the third section, RANS simulations of the aforementioned experiments are presented. Obtained numerical results are discussed in the fourth section, followed by conclusions.

Strained laminar flames

To evaluate major characteristics of critically perturbed laminar flames, strained planar flames are selected in the present work following Kuznetsov and Sabelnikov [34]. The same model problem was addressed by Venkateswaran et al. [30,31] and by Zhang et al. [32] to parameterize their experimental data. The problem involves two identical adiabatic, axially symmetric laminar premixed flames stabilized using opposed jets, see Fig. 1. Due to the symmetry of the problem with respect to the stagnation plane, a single flame is simulated. Such a problem is commonly modeled [56,57] with a set of stationary, one-dimensional, axially symmetric transport equations for concentrations of various species and the mixture enthalpy (internal energy, or temperature), supplemented with (i) continuity and impulse equations, (ii) a state equation, (iii) a model of molecular transport, and (iv) a chemical mechanism.

In the present work, these standard equations were numerically solved by running the module OPPDIF [57] of CHEMKIN-II software [58] and activating options *Multicomponent* and *Thermal Diffusion*. When simulating weakly strained flames, the parameters GRAD and CURV, which controlled the spatial resolution, were set equal to 0.05 each. At high strain rates close to extinction points, these parameters were decreased to obtain converged results that were weakly sensitive to a further decrease in GRAD or CURV. Typically, both parameters were equal to 0.005 and the number of grid points was about 5000. In a few cases, GRAD and CURV were as small as 0.003, with the number of grid points being about 15 000.

Distance between the inlet boundary (associated with a nozzle in Fig. 1) and the stagnation plane was set equal to 10 mm. The strain rate κ, which was equal to the stretch rate for the studied planar flames, was changed by varying the inlet flow velocity and was characterized using the local peak absolute value of the axial gradient of the axial flow velocity, reached upstream of the reaction zone. The laminar consumption velocity S_c was evaluated by integrating the heat release rate along the normal to the flame. The major goal of the simulations consisted in finding the peak values S_c^{max} of the computed dependencies of $S_c(\kappa)$. As shown in Fig. 2a,
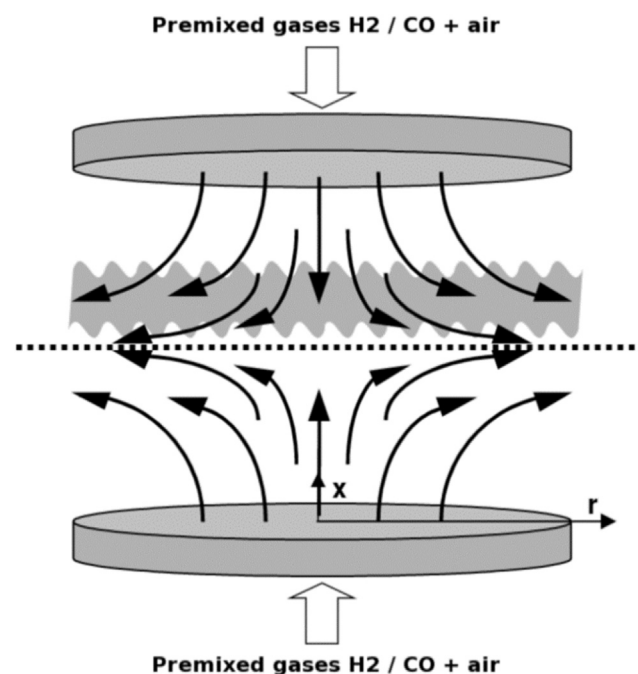

Fig. 1 — **Strained laminar premixed flames stabilized in opposed jets.**
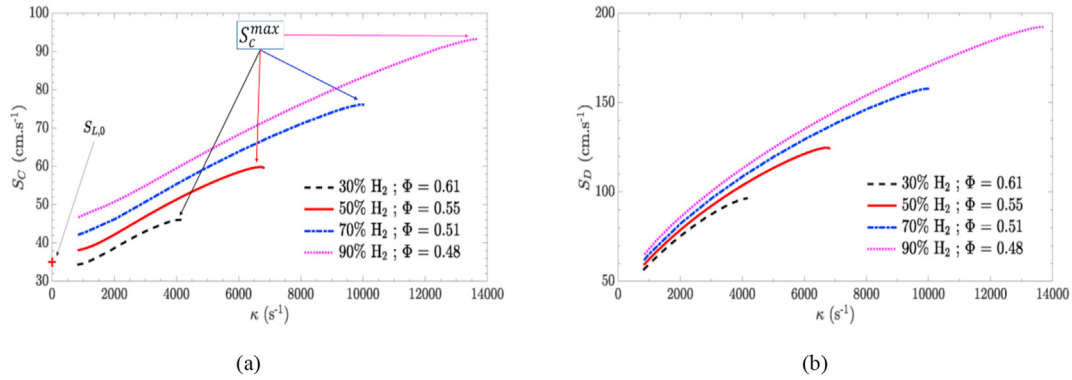
(a)　　　　　　　　　　　　　　　　(b)

Fig. 2 – Dependencies of (a) the consumption velocity S_c and (b) the flame displacement speed S_d computed for strained H_2/CO/air laminar flames under the room conditions. Φ designates the equivalence ratio.

these peak values were reached close to the flame extinction point κ_q.

It is worth noting that Fig. 2a differs from Fig. 16 in Ref. [30], where results of similar simulations performed for the same mixtures are shown. The point is that Venkateswaran et al. [30] reported a flame displacement speed S_d, which was equal to "*the minimum velocity just ahead of the reaction zone*" in their study. In the unperturbed laminar flame, the consumption velocity and displacement speed are equal to one another, with this identity being checked in the present study. However, in a strained laminar flame, $S_c \neq S_d$ [37–39]. Indeed, the minimum flow velocities S_d just ahead of the reaction zone, computed by us and shown in Fig. 2b, differ significantly from the consumption velocities evaluated under the same conditions, with the present dependencies of $S_d(\kappa)$ being similar to the aforementioned numerical results by Venkateswaran et al. [30]. Some differences still remain probably due to the use of different chemical mechanisms. The point is that Venkateswaran et al. [30] adopted a chemical mechanism by Davis et al. [59], whereas a more recent mechanism by Goswami et al. [60] is selected in the present paper. For the same reason, the unperturbed laminar flame speeds S_L obtained in the present work, see Table 1, differ slightly from the values of S_L reported by Venkateswaran et al. [30] and reproduced in Tables 2 and 3 in the next section.

In a single case (the pressure $P = 1$ atm and the volumetric H_2/CO ratio is equal to 50/50, with all results reported in the present manuscript being obtained for the unburned gas temperature equal to 300 K), two other recent chemical mechanisms by Kéromnès et al. [61] and by Li et al. [62] were also probed. Dependencies of $S_c(\kappa)$ computed using these three mechanisms looked similar, but the values of κ_q and S_c^{max} were slightly different. More precisely, the peak values S_c^{max} of

the laminar consumption velocity obtained using these three mechanisms are equal to 0.60, 0.62, and 0.63 m/s in that case.

The ratios of S_c^{max}/S_L, computed for all H_2/CO/air mixture compositions studied in the Atlanta experiments [30,31] are reported in Table 1. In line with the leading point concept, these values were used as input parameters for RANS simulations of turbulent premixed flames, discussed in the next section.

Finally, Fig. 3 shows a typical dependence of $S_c(\kappa)$, computed at low strain rates. The dependence changes drastically at $\kappa \to 0$ (and, hence, $S_c \to S_L$), thus, indicating that the Markstein number $Ma_c = \delta_L^{-1}(dS_c/d\kappa)_{\tau_c \kappa \to 0}$ is not appropriate for describing significant differences between $S_c(\kappa)$ and S_L at moderate (and high) strain rates. Accordingly, the use of Ma_c for modeling strong variations in local burning rate in turbulent flows does not seem to be appropriate either. Note, that figures similar to Fig. 3 are reported in other experimental and numerical papers, e.g. see Ref. [63].

Turbulent flames

Studied cases

Experiments simulated by us were performed using conical H_2/CO/air turbulent flames stabilized at the burner nozzle [30,31,64]. Two nozzles with diameters D equal to 12 and 20 mm were utilized. The unburned gas temperature was equal to 300 K, whereas the pressure P was changed from 1 to 10 atm. The volumetric H_2/CO ratio was varied from 30/70 to 90/10. The flow characteristics were changed by varying (i) the mean inlet flow velocity U from 4 to 50 m/s and/or (ii) blockage ratio (BR) for a plate located upstream of the nozzle [64]. Consequently, the rms turbulent velocity u', measured at the flow centerline 1 mm above the nozzle, was varied from 0.4 m/

Table 1 – Increase in the consumption velocity in extremely strained laminar flames.													
H_2, %	30	30	30	30	50	50	50	60	60	60	70	70	90	90
Φ	0.61	0.70	0.80	0.75	0.55	0.68	0.75	0.4	0.6	0.8	0.51	0.63	0.48	0.59
P, atm	1	1	1	5	1	5	10	1	1	1	1	5	1	5
S_L, m/s	0.36	0.47	0.59	0.35	0.35	0.36	0.35	0.14	0.49	0.88	0.35	0.36	0.35	0.37
κ_q, ms^{-1}	4.2	5.55	7.1	26.7	6.6	47.6	96.1	1.3	10.7	16.4	10.0	75.2	13.7	106.
S_c^{max}/S_L	1.28	1.19	1.14	1.37	1.71	1.86	1.81	3.0	1.67	1.28	2.17	2.44	2.66	3.0

Table 2 – Variations of equivalence ratio.

N	H_2, %	Φ	S_L, m/s	U, m/s	$\sqrt{2k}/S_L$	D, mm	P, atm
1	30	0.61, 0.70, 0.80	0.34, 0.48, 0.59	50	33, 25, 20	20	1
2	30	0.61, 0.70, 0.80	0.34, 0.48, 0.59	30	17, 13, 10	20	1
3	60	0.40, 0.60, 0.80	0.15, 0.51, 0.90	50	82, 24, 13	20	1
4	60	0.40, 0.60, 0.80	0.15, 0.51, 0.90	30	43, 13, 7.0	20	1

Table 3 – Variations of hydrogen concentration in the fuel blend at a constant laminar flame speed.

N	H_2, %	Φ	S_L, m/s	U, m/s	$\sqrt{2k}/S_L$	D, mm	P, atm
1	30, 50, 70, 90	0.61, 0.55, 0.51, 0.48	0.34	50	33	20	1
2	30, 70, 90	0.61, 0.51, 0.48	0.34	50	21	12	1
3	30, 50, 70, 90	0.75, 0.68, 0.63, 0.59	0.34	50	21	12	5
4	30, 50, 70, 90	0.61, 0.55, 0.51, 0.48	0.34	30	17	20	1
5	30, 50, 70, 90	0.61, 0.55, 0.51, 0.48	0.34	30	13	12	1
6	30, 50, 70	0.75, 0.68, 0.63	0.34	30	13	12	5
7	50	0.75	0.34	30	13	12	10
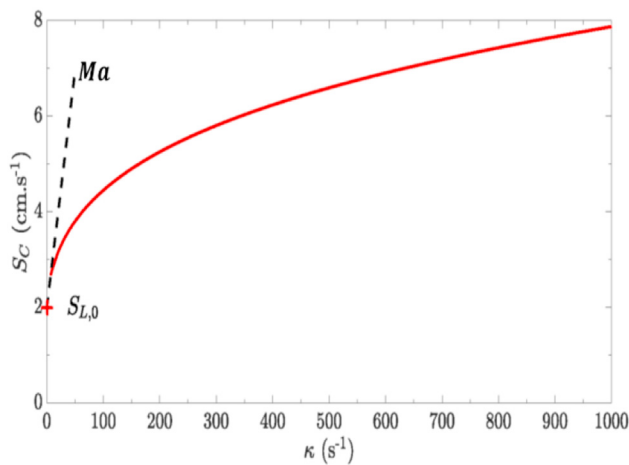
Fig. 3 – A typical dependence of the consumption velocity S_c on the strain rate computed for weakly strained lean H_2/CO/air laminar flames. 50% H_2 and 50% CO, $\Phi = 0.4, P = 10$ atm.

s (U = 4 m/s and BR = 69%) to 9 m/s (U = 50 m/s and BR = 93%) [64]. The measured longitudinal integral length scale L of the incoming turbulence was mainly controlled by the diameter D, but depended also on U and BR (0.05 < L/D < 0.3, see Fig. 13 in Ref. [64]).

For a single nozzle, a single mixture composition, and a single P, totally 52 different incoming flows were studied (13 different BRs and four different U) in the experiments [30,31]. For three different pressures, two different nozzles, and nine different mixture compositions, the entire condition matrix is five-dimensional and contains about 2800 cells. While not all these cells were filled in the Atlanta experiments [30,31], the number of the reported turbulent consumption velocities is still larger than 500. Accordingly, we had to reduce the condition matrix in order to make the simulations and analysis of their results feasible. Since the present study aims primarily at effects due to variation of the hydrogen amount in highly turbulent lean H_2/CO/air flames, we (i) restricted ourselves to

the two highest inlet flow velocities (U = 30 and 50 m/s), but (ii) simulated all mixtures and pressures for which the turbulent burning velocity U_T was measured by Venkateswaran et al. [30,31]. Moreover, since the influence of turbulence length scale on burning rate is understood worse than the influence of u' on U_T [65], but can be of great importance [66], the experiments with both nozzles were simulated. Furthermore, to make the simulations feasible and analysis of results clear, we restricted ourselves to a single representative BR of 81%, which was the median value of the interval of BRs investigated by Venkateswaran et al. [30,31]. This restriction was also set for the following two reasons.

First, variations of U and BR in the experiments changed not only u' and L, but other turbulence characteristics also. For instance, turbulence spectra shown in Figs. 14 and 15 in Ref. [64] are different for different BRs or different U, respectively. Accordingly, without detailed simulations of the flow through the plate and near the walls of the contoured nozzle used in the experiments, the inlet turbulence cannot be properly characterized. Since such complicated simulations of confined turbulent inert flows are beyond the scope of the present study, the inlet boundary conditions were set by us at the nozzle exit. However, for turbulence characteristics, such boundary conditions are poorly known. In particular, the "constant" C_d in Eq. (9) discussed later could be different for each pair of U and BR. Consequently, this "constant" may be tuned for each pair of U and BR. However, such tuning is of minor interest for the goals of the present study.

Second, as reviewed elsewhere [65,67], capabilities of the Turbulent Flame Closure (TFC) model [68,69] used in the present work for predicting dependencies of turbulent burning velocity U_T on u' were already documented by various research groups in RANS simulations of different experiments performed under substantially different conditions. Accordingly, one more such test of the TFC model is of secondary interest, especially as a solid test is impeded due to the aforementioned problem of the inlet boundary conditions.

Thus, for the above reasons, the present numerical study was restricted to a single BR. For this BR, the ratio of L/D is close to 0.1. Conditions of the experiments simulated in the

present paper are summarized in Tables 2 and 3 for series of measurements performed by varying the equivalence ratio Φ and H_2/CO ratio, respectively. There, $k = 3u'^2/2$ is turbulent kinetic energy. Note that the values of the laminar flame speed, reported in these two tables, are taken from Refs. [30,31], whereas slightly different values of S_L, see Table 1, were adopted in the present RANS computations.

Combustion model

In the present work, the so-called TFC model [68,69] of the influence of turbulence on premixed combustion is used for the following two major reasons. First, it is the sole model that has yet been adopted jointly with the leading point concept to predict abnormally high turbulent burning velocities [42] documented in very lean hydrogen-air turbulent flames. It is worth remembering, however, that those simulations [42] were performed for a single fuel (hydrogen) by invoking a single-step chemistry. Second, as reviewed elsewhere [35,65,67], the TFC model was quantitatively validated by several independent research groups in RANS simulations of various measurements done by burning substantially different hydrocarbon-air mixtures under a wide range of significantly different conditions. For instance, two of the present authors [70,71] successfully exploited the TFC model to simulate seven sets of experimental investigations of statistically stationary premixed turbulent flames whose geometrical configurations were different.

The TFC model is based on the following transport equation

$$\frac{\partial}{\partial t}(\bar{\rho}\tilde{c}) + \nabla \cdot (\bar{\rho}\tilde{\mathbf{u}}\tilde{c}) = \nabla \cdot (\bar{\rho}D_T\nabla\tilde{c}) + \rho_u U_T|\nabla\tilde{c}| \qquad (1)$$

for the Favre-averaged combustion progress variable $\tilde{c}$, which characterizes the thermochemical state of a reacting mixture in a flame and is equal to zero or unity in reactants or products, respectively. Here, t is the time; $\bar{\rho}$ is the mean density calculated by invoking the well-known Bray-Moss-Libby (BML) equations [72,73].

$$\bar{\rho} = \frac{\rho_u}{1 + (\sigma - 1)\tilde{c}}, \qquad \bar{\rho}\tilde{c} = \rho_b\bar{c}; \qquad (2)$$

$\mathbf{u}$ is the flow velocity vector; D_T and U_T are the turbulent diffusivity and burning velocity, respectively, discussed later; $\sigma = \rho_u/\rho_b$ is the density ratio; over-lines designate the Reynolds average, while $\tilde{q} = \overline{\rho q}/\bar{\rho}$ is the Favre-averaged value of q with $q'' = q - \tilde{q}$; subscripts u and b designate unburned reactants and burned products, respectively.

Eq. (1) written in another form was put forward by Prudnikov [74] who addressed statistically one-dimensional, planar premixed flames propagating in frozen turbulence. In the same simplified case, Eq. (1) was later derived by Lipatnikov and Chomiak [75] who studied a developing premixed turbulent flame with self-similar mean structure, as the self-similarity of the mean structure of developing premixed turbulent flames was well documented in various experiments, as reviewed elsewhere [35,65,74,76,77]. Eq. (1) is applicable to modeling premixed turbulent combustion in an intermediately asymptotic regime that is characterized by a stationary (to the leading order) turbulent burning velocity U_T but growing mean flame brush thickness δ_T. Such a regime of

turbulent burning was first pointed out by Prudnikov [74]. Later, the same regime was discussed by Kuznetsov [78], Clavin and Williams [79], and Zimont [80] who introduced the notion of "intermediate steady propagation (ISP) flames" [81].

To close Eq. (1), a model for the turbulent burning velocity U_T should also address the ISP regime of premixed combustion, i.e. turbulent flames with growing δ_T. The present authors are aware on the sole model that satisfies this consistency requirement. That model was developed by Zimont [80] and resulted in the following expression

$$U_T = Au'Da^{1/4} = Au'\left(\frac{\tau_T}{\tau_f}\right)^{1/4} = Au'\left(\frac{LS_L^2}{u'a_u}\right)^{1/4}. \qquad (3)$$

Here, $A = 0.5$ [69] is the sole constant of the TFC model; $Da = \tau_T/\tau_f$ is the Damköhler number; $\tau_f = a_u/S_L^2$ and $\tau_T = L/u'$ are the laminar-flame and turbulence time scales, respectively; and a_u is the molecular heat diffusivity of unburned reactants.

Zimont [80] derived Eq. (3) in the case of (i) a high turbulent Reynolds number, i.e. $Re_t = u'L/\nu_u \gg 1$, (ii) a high Damköhler number, i.e. $Da \gg 1$, and (iii) a large Karlovitz number, i.e. $Ka = Re_t^{1/2}/Da > 1$. Here, ν_u is the kinematic viscosity of unburned mixture. Moreover, in the regime explored by Zimont [80], the flame-development time should satisfy a constraint of $\tau_T < t_{fd} \ll \tau_T Da$. That derivation was based on the following three assumptions. First, the influence of small-scale turbulent eddies on combustion was reduced to increasing heat and mass transfer within local flames and thickening them, with the width of the thickened flames being significantly smaller than the integral length scale L. Second, the influence of large-scale turbulent eddies on combustion was reduced to wrinkling the thickened flame surface. Third, the flame brush thickness δ_T was considered to grow following the turbulent diffusion law. This hypothesis was earlier put forward by Karlovitz et al. [82] and was confirmed by numerous experimental data analyzed by Prudnikov [74]. Later, Lipatnikov and Chomiak [65] noted that the first aforementioned assumption could be changed to a more general assumption that the interaction between the local flame and the small-scale turbulent eddies was solely controlled by the flame time scale τ_f and the mean dissipation rate $\tilde{\varepsilon}$. This hypothesis, which is in fact an extension of the well-recognized Kolmogorov hypothesis to the case of premixed turbulent burning, allows us to substitute the constraint of $Ka > 1$ with a constraint of $u'/S_L > 1$, thus, making Eq. (3) applicable also to moderately turbulent combustion.

Subsequently, the TFC model was extended [83,84] (i) to yield a fully developed flame with a stationary thickness δ_T at large flame development time, i.e. $t_{fd}/\tau_T \to \infty$, and to address (ii) an earlier stage of flame development, i.e. $t_{fd} < \tau_T$, and (iii) the case of $u'/S_L < 1$. When simulating the Atlanta experiments studied in the present work, both the TFC model and its extension known as Flame Speed Closure (FSC) model yield close results, as in earlier simulations [70] of other confined Bunsen flames investigated experimentally in PSI [28,29]. Accordingly, the TFC model is adopted in the present work, because its joint use with the leading point concept requires a single simple change: the unperturbed laminar flame speed S_L

in Eq. (3) should be substituted with the peak consumption velocity S_c^{max} obtained from the critically strained laminar flame and reported in Table 1. Thus, in the present work, Eq. (3) is substituted with

$$U_T = Au' \left(\frac{L S_L^2}{u' a_u} \right)^{1/4} \left(\frac{S_c^{max}}{S_L} \right)^{1/2} = Au' Da^{1/4} \left(\frac{S_c^{max}}{S_L} \right)^{1/2}, \qquad (4)$$

where a factor of $(S_c^{max}/S_L)^{1/2}$ is constant within any premixed turbulent flame and can be pre-computed by adopting a detailed chemical mechanism, see Table 1. In a similar simple way, the leading point concept can be coupled with most models of premixed turbulent combustion used not only in RANS computations, but also in Large Eddy Simulations (LES).

It is worth stressing that the consumption velocity S_c characterizes burning rate in a perturbed laminar premixed flame much better than a displacement speed S_d does. The latter quantity is well known to be sensitive to the choice of an iso-scalar surface associated with the flame surface [39,40]. For instance, under certain conditions $\rho_u S_L$ can be larger (smaller) than ρS_d for one (another) iso-scalar surface within the same flame [39,40]. Moreover, a flame ball [33] is characterized by $S_d = 0$ for any iso-scalar surface, whereas the local burning rate per unit ball-surface area can be very high, i.e. $S_c \gg S_L$, in a very lean hydrogen-air mixture. Therefore, the peak consumption velocity S_c^{max} appears to be better suited for characterizing the local burning rate in the leading points when compared to a displacement speed.

Finally, to allow for entrainment of surrounding air into a conical flame, the following well-known transport equation

$$\frac{\partial}{\partial t}(\bar{\rho}\tilde{f}) + \nabla \cdot (\bar{\rho}\tilde{\mathbf{u}}\tilde{f}) = \nabla \cdot (\bar{\rho} D_T \nabla \tilde{f}) \qquad (5)$$

for the Favre-averaged mixture fraction $\tilde{f}$ [44—46] was numerically integrated, with Da in Eq. (4) being evaluated by substituting the obtained field $\tilde{f}(\mathbf{x})$ into the dependence of $S_L(f, H_2/CO, P)$, pre-computed for the unperturbed laminar flames using CHEMKIN-II [58] and the detailed chemical mechanism by Goswami et al. [60]. These simulations also yielded $\rho_b(f, H_2/CO, P)$ required to calculate the mean density adopting the BML Eq. (2).

Turbulence model
Modeling turbulence in a premixed flame still challenges the research community, with even characterization of turbulence in a flame being an issue [85]. As reviewed elsewhere [86,87], a number of local phenomena associated with the influence of thermal expansion on turbulence in a flame have been found in recent studies. Nevertheless, majority of these phenomena are not addressed by turbulence models used in RANS CFD research into premixed combustion. The use of LES does not resolve the problem either, because flame-turbulence interaction is mainly localized to small scales that are not resolved in a typical LES [88]. Even if the discussed thermal expansion effects could be of less importance in highly turbulent premixed flames, predictive capabilities of available turbulence models have to be documented in such flames. However, this task has yet been rarely (if ever) addressed.

In our earlier tests [70,71] of the TFC and FSC models, the issue of simulating turbulence in premixed flames was partially circumvented in the following way. For each set of simulated experiments, (i) a single reference case was chosen, (ii) several turbulence models and relevant inlet boundary conditions were probed to get the best agreement with data measured in that single case, and (iii) the best model and boundary conditions were subsequently used to explore other experiments from the studied set. Note that the single constant A of the TFC or FSC model was not tuned in Refs. [70,71].

The same method could also be used in the present work, but because its focus was placed on the influence of $H_2/CO/air$ mixture composition and pressure on turbulent burning velocity, a simpler and less expensive solution was taken. More specifically, the well-known $k - \varepsilon$ model of turbulence [89], extended based on the Rapid Distortion Theory [90], was adopted. The model involves the following two transport equations

$$\frac{\partial}{\partial t}(\bar{\rho}\tilde{k}) + \frac{\partial}{\partial x_k}\left(\bar{\rho}\tilde{u}_k\tilde{k}\right) = \nabla \cdot \left(\bar{\rho}\frac{\nu_T}{\sigma_k}\frac{\partial \tilde{k}}{\partial x_k}\right) - \bar{\rho}\widetilde{u_j'' u_k''}\frac{\partial \tilde{u}_j}{\partial x_k} - \bar{\rho}\tilde{\varepsilon}, \qquad (6)$$

$$\frac{\partial}{\partial t}(\bar{\rho}\tilde{\varepsilon}) + \frac{\partial}{\partial x_k}\left(\bar{\rho}\tilde{u}_k\tilde{\varepsilon}\right) = \nabla \cdot \left(\bar{\rho}\frac{\nu_T}{\sigma_\varepsilon}\frac{\partial \tilde{\varepsilon}}{\partial x_k}\right) - C_{\varepsilon,1}\frac{\tilde{\varepsilon}}{\tilde{k}}\bar{\rho}\widetilde{u_j'' u_k''}\frac{\partial \tilde{u}_j}{\partial x_k} - C_{\varepsilon,2}\bar{\rho}\frac{\tilde{\varepsilon}^2}{\tilde{k}}$$
$$+ C_{\varepsilon,3}\bar{\rho}\tilde{\varepsilon}\frac{\partial \tilde{u}_k}{\partial x_k} \qquad (7)$$

for the Favre-averaged turbulent kinetic energy $\tilde{k} = \widetilde{u_k'' u_k''}/2$ and its dissipation rate $\tilde{\varepsilon}$. Here,

$$\nu_T = C_\mu \frac{\tilde{k}^2}{\tilde{\varepsilon}} \qquad (8)$$

is kinematic turbulent viscosity, $\sigma_k = 1.0$, $\sigma_\varepsilon = 1.3 C_\mu = 0.09$, $C_{\varepsilon,1} = 1.44$, and $C_{\varepsilon,2} = 1.92$ are standard constants of the $k - \varepsilon$ model [89], $C_{\varepsilon,3} = -1/3$ [90,91], and the summation convention applies to repeated indexes.

The inlet boundary conditions are set as follows

$$\tilde{\varepsilon} = C_d\frac{u'^3}{L} = C_d'\frac{\tilde{k}^{3/2}}{L}, \quad \tilde{k} = \frac{3}{2}u'^2, \qquad (9)$$

where $C_d = 0.3$ if $C_d' = C_\mu^{3/4}$ and $C_\mu = 0.09$. These values are default values in various CFD codes. The rms velocity $(u_{tot}' \equiv \sqrt{\overline{u'^2} + \overline{v'^2} + \overline{w'^2}} = \sqrt{3}u')$ and length scale L are reported in Figs. 10 and 13, respectively, in Ref. [64]. The turbulent diffusivity is evaluated as follows

$$D_T = \frac{C_\mu}{Sc_T}\frac{\tilde{k}^2}{\tilde{\varepsilon}}, \qquad (10)$$

with $Sc_T = 0.7$ [67].

Numerical setup
Unsteady numerical simulations were performed by using a significantly modified version of the XiFoam solver in the OpenFOAM CFD library [92] until a stationary solution was reached. The computational domain was two-dimensional in the cylindrical coordinate framework. The domain began at $x = -2D$, the inlet was placed at $x = 0$, and the domain size downstream of the inlet was equal to $25D \times 5D$. In a few representative cases, very similar results were obtained from

a bigger computational domain of size $50D \times 10D$ downstream of the inlet. The numerical mesh consisted of approximately 140 000 cells and had the smallest steps in the axial and radial directions equal to $\Delta x = 0.5$ mm and $\Delta r = 0.25$ mm, respectively. The steps were kept constant in the zone $x < 10D$ and $r < 2D$ and were then gradually increased with both the radial and axial distances from the nozzle exit, see Fig. 4. In a few representative cases, very similar results were computed using a finer mesh of approximately 320 000 cells with the minimum $\Delta x = 0.334$ mm and $\Delta r = 0.167$ mm.

Boundary conditions were set using options offered by the OpenFOAM library at different boundaries marked in Fig. 4. The conditions are summarized in Table 4 adopting names accepted in the OpenFOAM library. In the experiments, a pilot methane-air flame was used, "*with the total mass flow rate of the pilot*" being less than "*5% of the main flow rate*" [30]. However, the pilot-flame composition, mean inlet velocity, and pilot slot, burner rim, and pilot rim widths are not reported in Refs. [30,31,64]. In the present simulations, (i) the mean inlet velocity of the pilot flow was equal to $U/2$, (ii) $\tilde{f}$ was the same in the major flow of unburned reactants and in the pilot flow of combustion products, (iii) $\tilde{c} = 0$ and 1 in the two flows, respectively, (iv) the pilot slot thickness was equal to 2 mm, whereas thickness of wall 2 was equal to 1 mm. In a single representative case, either the pilot slot width or the mean inlet velocity was decreased by a factor of two independently from one another, but the computed turbulent burning velocities were almost the same in these test cases.

Target of simulations

In line with the experimental study, e.g. see Fig. 13b in Ref. [30], a bulk turbulent burning velocity is evaluated as follows
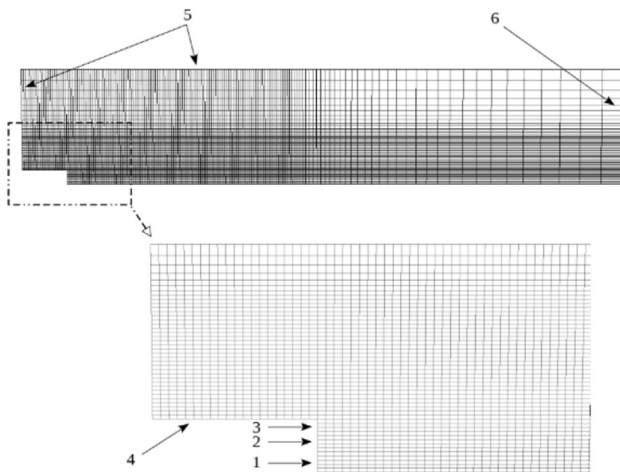

Fig. 4 – Computational mesh and boundary conditions. To improve readability of the figure, the number of shown grid points is decreased by a factor of four in both axial and radial direction. 1 – major flow inlet; 2 – rim; 3 – pilot flow; 4 – burner wall; 5 – entrainment boundaries; 6 – outlet boundary.

$$U_T = \frac{\dot{m}}{\rho_u A_f}, \tag{11}$$

$$A_f = \pi R \sqrt{R^2 + H_f^2}, \tag{12}$$

where $\dot{m}$ is the inlet mass flow rate, A_f is the area of the side surface of the mean flame cone, $R = D/2$ is the nozzle radius, and the mean flame height H_f is calculated using the constraint of $\bar{c}(r = 0, x = H_f) = 0.5$.

Contrary to the earlier tests [70,71] of the TFC and FSC models, the constant A in Eq. (4) was tuned here. More specifically, it was tuned in a single reference case (30% H_2, $\Phi = 0.61$, and $P = 1$ atm). Other flames were simulated by retaining the same values of all constants (A, σ_k, σ_ε, $C_{\varepsilon,1}$, $C_{\varepsilon,2}$, C_μ, C_d, and Sc_T). The tuned value of $A = 0.66$ is larger than the recommended value of $A = 0.5$. This tuned value could be reduced by decreasing C_d and/or Sc_T, but such exercises were beyond the scope of the present work. The discussed simplifications (the use of a default turbulence model with default boundary conditions and tuning the TFC constant A in a single reference case associated with the minimum amount of H_2 in the fuel blend) appear to be fully adequate for the major goal of the present study, which consists in assessing the capabilities of the TFC model combined with the leading point concept, i.e. Eq. (4), for predicting a substantial increase in turbulent burning velocity with increasing H_2/CO ratio by retaining the same S_L. It is worth stressing that such data measured by Venkateswaran et al. [30,31] still challenge the combustion CFD community and the present authors are not aware on a work where these experimental data are predicted in RANS computations or LES.

Results and discussion

A typical image of the computed field of the Favre-averaged temperature is shown in Fig. 5. The image looks similar to the experimental images, e.g. see Fig. 13b in Ref. [30]. Note that while the flame shape is not conical in the two aforementioned figures, Eqs. (11) and (12) were used in the present paper, because the same method was adopted to measure U_T [30].

Results of validation of the leading point concept combined with the TFC model, i.e. Eq. (4), are summarized in Figs. 6 and 7, where open symbols show simulated results and filled symbols show experimental data by Venkateswaran et al. [30,31]. More specifically, Fig. 6 aims at assessing the capability of the model to predict dependencies of U_T yielded by Eq. (11) on the equivalence ratio in lean flames with H_2/CO = 30/70 (diamonds and squares) or H_2/CO = 60/40 (circles and triangles) at two different values of the inlet velocity $U = 30$ m/s (squares and triangles) or 50 m/s (diamonds and circles). The corresponding values of u' are about 3.5 ad 6.8 m/s, respectively, i.e., significantly larger than the laminar flame speeds reported in Table 2. Note that (i) the laminar flame speeds are different for different mixtures plotted in Fig. 6 and (ii) open diamond and open square at $\Phi = 0.61$ show results computed by tuning A, i.e. increasing it to 0.66. Other computed results

Table 4 – Boundary conditions.

N	boundary	$\tilde{u}$	$\bar{p}$	$\tilde{c}$ or $\tilde{f}$	$\tilde{k}$	$\tilde{\varepsilon}$
1	inlet	fixedValue	zeroGradient	fixedValue	fixedValue	fixedValue
2	rim	fixedValue	zeroGradient	zeroGradient	zeroGradient	zeroGradient
3	pilot	fixedValue	zeroGradient	fixedValue	fixedValue	fixedValue
4	wall	fixedValue	zeroGradient	zeroGradient	compressible:: kqRWallFunction	compressible:: epsilonWallFunction
5	entrainment	zeroGradient	zeroGradient	zeroGradient	zeroGradient	zeroGradient
6	outlet	zeroGradient	totalPressure	zeroGradient	zeroGradient	zeroGradient
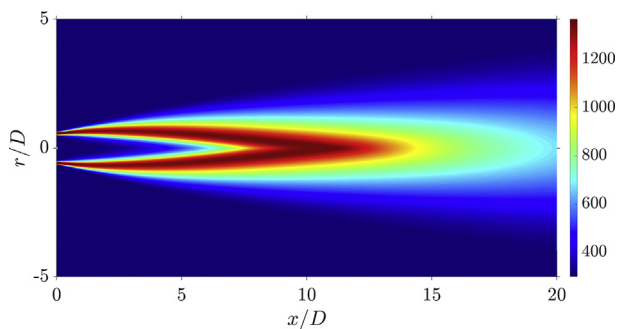
Fig. 5 – Field of the Favre-averaged temperature computed at P = 1 atm, D = 20 mm, U = 50 m/s, H2/CO = 60/40, Φ = 0.4.
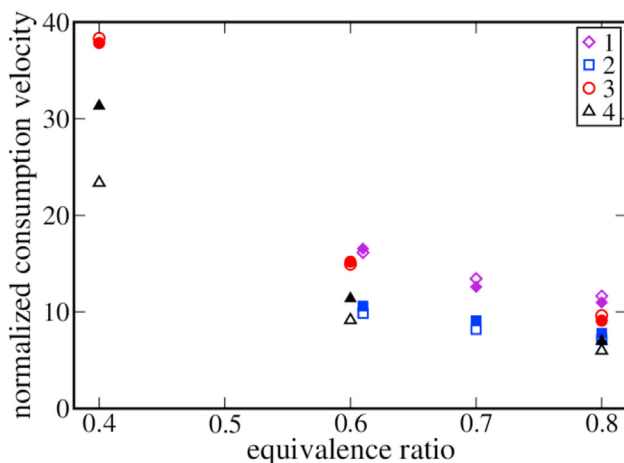
Fig. 6 – Dependence of the normalized consumption velocity U_T/S_L on the equivalence ratio Φ. Open and filled symbols show computed results and data measured by Venkateswaran et al. [30,31]. 1—30% H₂, U = 50 m/s, D = 20 mm, P = 1 atm; 2—30% H₂, U = 30 m/s, D = 20 mm, P = 1 atm; 3—60% H₂, U = 50 m/s, D = 20 mm, P = 1 atm; 4—60% H₂, U = 30 m/s, D = 20 mm, P = 1 atm.

Fig. 7 – Dependence of the normalized consumption velocity U_T/S_L on the amount of hydrogen in the fuel blend. Open and filled symbols show computed results and data measured by Venkateswaran et al. [30,31]. 1 – U = 50 m/s, D = 20 mm, P = 1 atm; 2 – U = 50 m/s, D = 12 mm, P = 1 atm; 3 – U = 50 m/s, D = 12 mm, P = 5 atm; 4 – U = 30 m/s, D = 20 mm, P = 1 atm; 5 – U = 30 m/s, D = 12 mm, P = 1 atm; 6 – U = 30 m/s, D = 12 mm, P = 5 atm; 7 – U = 30 m/s, D = 12 mm, P = 10 atm. Other conditions are specified in Table 3.

Fig. 7 aims at assessing the capability of the tested model for predicting a significant (by a factor up to 1.5) increase in U_T when increasing the H₂/CO ratio, but retaining the same value of $S_L = 0.34$ m/s [30]. This experimental finding challenges state-of-the-art models of premixed turbulent combustion. The studied cases cover two different U = 30 and 50 m/s, two different nozzle diameters (and, hence, two significantly different integral length scales of the turbulence), three different pressures P = 1, 5, and 10 atm, and $0.48 \leq \Phi \leq 0.75$, see Table 3. All in all, the obtained agreement between the measured and computed turbulent burning velocities is encouraging. The worst agreement is observed in the cases of (i) H₂/CO = 30/70, U = 50 m/s, P = 1 atm, D = 12 mm, cf. filled and open squares, (ii) H₂/CO = 70/30, U = 30 m/s, D = 20 mm, P = 1 atm, cf. filled and open up-pointing triangles, and (iii) H₂/CO = 90/10, U = 30 m/s, D = 20 mm, P = 1 atm, cf. filled and open up-pointing triangles. In these three cases, the model overestimates, see (i), or underestimates, see (ii) and (iii), U_T by 20—25% approximately. In other 20 cases, including all high-pressure cases, the measured and computed results appear to agree sufficiently well. It is worth

reported in Fig. 6 have been obtained without additional tuning, i.e. A = 0.66 in all cases. Fig. 6 quantitatively validates the model in all cases with the exception of a single case of H₂/CO = 60/40, U = 30 m/s, and Φ = 0.4, cf. open and filled triangles. In this single case, the model significantly (about 25%) underestimates the measured burning velocity and the reasons for this are unclear.
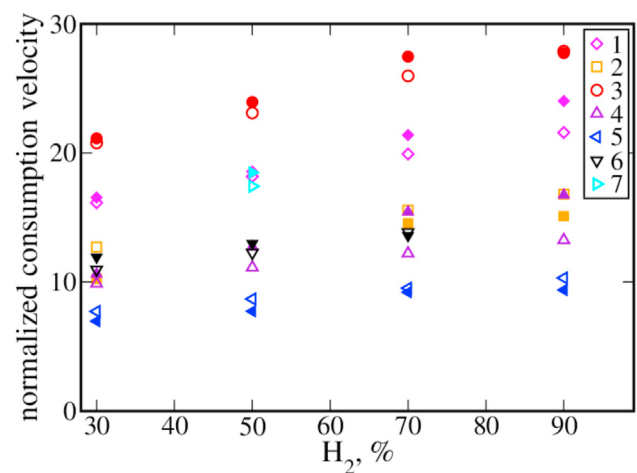
stressing that the same value of $A = 0.66$ was used in all these simulations. Therefore, the significant effect of the H_2/CO ratio on U_T is predicted due to the use of the term $(S_c^{max}/S_L)^{1/2}$ in Eq. (4), based on the leading point concept. Bearing in mind the wide range of the studied mixture compositions and pressures, results reported in Figs. 6 and 7 indicate that the tested approach, i.e. the leading point concept combined with the TFC model, in particular Eq. (4), is capable for predicting well-pronounced diffusional-thermal effects in lean highly turbulent syngas-air flames. Accordingly, Eq. (4) may be recommended for CFD research into turbulent burning of lean syngas-air mixtures, with this equation being compatible not only with various RANS, but also with various LES models of the influence of turbulence on premixed combustion.

Conclusions

The Turbulent Flame Closure (TFC) model of the influence of turbulence on premixed burning was combined with the leading point concept in order to allow for diffusional-thermal effects in premixed turbulent flames. The combined model was tested in RANS simulations of highly turbulent, lean syngas-air flames that were experimentally investigated by Venkateswaran et al. [30,31]. The tests were performed for four different values of the inlet rms turbulent velocity u', different turbulence length scales L, normal and elevated (up to 10 atm) pressures, various H_2/CO ratios ranging from 30/70 to 90/10, and various equivalence ratios $0.40 \leq \Phi \leq 0.80$. In 28 of the studied 33 cases, including all high-pressure flames, the computed bulk turbulent consumption velocities agree quantitatively with the experimental data, with these results being obtained using the same value of a single constant of the tested approach. In five other cases, differences are about 20–25%. All in all, the performed tests indicate that the studied combination of the leading point concept and the TFC model, in particular Eq. (4), is capable for predicting well-pronounced diffusional-thermal effects in lean highly turbulent syngas-air flames. For instance, the combined model well predicts a significant increase in the bulk turbulent consumption velocity when increasing the H_2/CO ratio but retaining the same value of the laminar flame speed.

Declaration of competing interest

The authors declare that they have no known competing financial interests or personal relationships that could have appeared to influence the work reported in this paper.

Acknowledgements

REFERENCES

[1] Verhelst S, Wallner T. Hydrogen-fueled internal combustion engines. Prog Energy Combust Sci 2009;35:490–527.

[2] Dinkelacker F, Manickam B, Muppala SPR. Modelling and simulation of lean premixed turbulent methane/hydrogen/air flames with an effective Lewis number approach. Combust Flame 2011;158:1742–9.

[3] Xie Y, Sun ZY. Effects of the external turbulence on centrally-ignited spherical unstable CH_4/H_2/air flames in the constant-volume combustion bomb. Int J Hydrogen Energy 2019;44:20452–61.

[4] Akansu SO, Dulger Z, Kahraman N, Veziroglu TN. Internal combustion engines fueled by natural gas-hydrogen mixtures. Int J Hydrogen Energy 2004;29:1527–39.

[5] Hu EJ, Huang ZH, Liu B, Zheng JJ, Gu XL. Experimental study on combustion characteristics of a spark-ignition engine fueled with natural gas-hydrogen blends combining with EGR. Int J Hydrogen Energy 2009;34:1035–44.

[6] Ma FH, Wang YF, Ding SF, Jiang L. Twenty percent hydrogen-enriched natural gas transient performance research. Int J Hydrogen Energy 2009;34:6523–31.

[7] Zhang M, Chang M, Wang J, Huang Z. Flame dynamics analysis of highly hydrogen-enrichment premixed turbulent combustion. Int J Hydrogen Energy 2020;45(1):1072–83.

[8] Aravind B, Kishore VR, Mohammad A. Combustion characteristics of the effect of hydrogen addition on LPG-air mixtures. Int J Hydrogen Energy 2015;40:16605–17.

[9] Pan W, Liu D. Effects of hydrogen additions on premixed rich flames of four butanol isomers. Int J Hydrogen Energy 2017;42(6):3833–41.

[10] Yu X, Li G, Du Y, Guo Z, Shang Z, He F, Shen Q, Li D, Li Y. A comparative study on effects of homogeneous or stratified hydrogen on combustion and emissions of a gasoline/hydrogen SI engine. Int J Hydrogen Energy 2019;44:25974–84.

[11] Montoya JPG, Amell A, Olsen DB, Diaz GJA. Strategies to improve the performance of a spark ignition engine using fuel blends of biogas with natural gas, propane and hydrogen. Int J Hydrogen Energy 2018;43:21592–602.

[12] Hu Z, Zhang X. Experimental study on flame stability of biogas/hydrogen combustion. Int J Hydrogen Energy 2019;44:5607–14.

[13] Wei Z, He Z, Zhen H, Zhang X, Chen Z, Huang Z. Kinetic modeling investigation on the coupling effects of H_2 and CO_2 addition on the laminar flame speed of hydrogen enriched biogas mixture. Int J Hydrogen Energy 2020;45(51):27891–903. https://doi.org/10.1016/j.ijhydene.2020.07.119.

[14] Richards GA, Casleton KH. Gasification technology to produce synthesis gas. In: Lieuwen TC, Yang V, Yetter RA, editors. Synthesis gas combustion: fundamentals and applications. CRC Press; 2009. p. 1–28.

[15] Tahtouh T, Halter F, Mounaïm-Rousselle C. Laminar premixed flame characteristics of hydrogen blended isooctane-air-nitrogen mixtures. Int J Hydrogen Energy 2011;36(1):985–91.

[16] Varghese RJ, Kumar S. Machine learning model to predict the laminar burning velocities of H_2/CO/CH_4/CO_2/N_2/air mixtures at high pressure and temperature conditions. Int J Hydrogen Energy 2020;45(4):3216–32.

[17] Jithin EV, Varghese RJ, Velamati RK. Experimental and numerical investigation on the effect of hydrogen addition and N_2/CO_2 dilution on laminar burning velocity of methane/oxygen mixtures. Int J Hydrogen Energy 2020;45:16838–50.

[18] Nakahara M, Kido H. Study on the turbulent burning velocity of hydrogen mixtures including hydrocarbon. AIAA J 2008;46:1569–75.

[19] Muppala SPR, Nakahara M, Aluri NK, Kido H, Wen JX, Papalexandris MV. Experimental and analytical investigation of the turbulent burning velocity of two-component fuel mixtures of hydrogen, methane and propane. Int J Hydrogen Energy 2009;34:9258–65.

[20] Chiu CW, Dong YC, Shy SS. High-pressure hydrogen/carbon monoxide syngas turbulent burning velocities measured at constant turbulent Reynolds numbers. Int J Hydrogen Energy 2012;37(14):10935–46.

[21] Mansouri Z, Aouissi M, Boushaki T. Numerical computations of premixed propane flame in a swirl-stabilized burner: effects of hydrogen enrichment, swirl number and equivalence ratio on flame characteristics. Int J Hydrogen Energy 2016;41(22):9664–78.

[22] Ranga Dinesh KKJ, Shalaby H, Luo KH, van Oijen JA, Thévenin D. High hydrogen content syngas fuel burning in lean premixed spherical flames at elevated pressures: effects of preferential diffusion. Int J Hydrogen Energy 2016;41(40):18231–49.

[23] Cecere D, Giacomazzi E, Arcidiacono NM, Picchia FR. Direct numerical simulation of high pressure turbulent lean premixed CH_4/H_2-air slot flames. Int J Hydrogen Energy 2018;43(10):5184–98.

[24] Zhang GP, Li GX, Li HM, Jiang YH, Lv JC. Experimental investigation on the self-acceleration of $10\%H_2/90\%CO$/air turbulent expanding premixed flame. Int J Hydrogen Energy 2019;44:24321–30.

[25] Huang K, Sun ZY, Tian YC, Wang KL. Turbulent combustion evolution of stoichiometric H_2/CH_4/air mixtures within a spherical space. Int J Hydrogen Energy 2020;45:10613–22.

[26] Lipatnikov AN, Chomiak J. Molecular transport effects on turbulent flame propagation and structure. Prog Energy Combust Sci 2005;31(1):1–73.

[27] Yang S, Saha A, Liang W, Wu F, Law CK. Extreme role of preferential diffusion in turbulent flame propagation. Combust Flame 2018;188:498–504.

[28] Daniele S, Jansohn P, Mantzaras J, Boulouchos K. Turbulent flame speed for syngas at gas turbine relevant conditions. Proc Combust Inst 2011;33:2937–44.

[29] Daniele S, Mantzaras J, Jansohn P, Denisov A, Boulouchos K. Flame front/turbulence interaction for syngas fuels in the thin reaction zones regime: turbulent and stretched laminar flame speeds at elevated pressures and temperatures. J Fluid Mech 2013;724:36–68.

[30] Venkateswaran P, Marshall A, Shin DH, Noble D, Seitzman J, Lieuwen T. Measurements and analysis of turbulent consumption speeds of H_2/CO mixtures. Combust Flame 2011;158:1602–14.

[31] Venkateswaran P, Marshall A, Seitzman J, Lieuwen T. Pressure and fuel effects on turbulent consumption speeds of H_2/CO blends. Proc Combust Inst 2013;34:1527–35.

[32] Zhang W, Wang J, Yu Q, Jin W, Zhang M, Huang Z. Investigation of the fuel effects on burning velocity and flame structure of turbulent premixed flames based on leading points concept. Combust Sci Technol 2018;190:1354–76.

[33] Zel'dovich YaB, Barenblatt GI, Librovich VB, Makhviladze GM. The mathematical theory of combustion and explosions. Consultants Bureau; 1985.

[34] Kuznetsov VR, Sabelnikov VA. Turbulence and combustion. Hemisphere; 1990.

[35] Lipatnikov AN. Fundamentals of premixed turbulent combustion. CRC Press; 2012.

[36] Day MS, Bell JB, Cheng RK, Tachibana S, Beckner VE, Lijewski MJ. Cellular burning in lean premixed turbulent hydrogen-air flames: coupling experimental and computational analysis at the laboratory scale. J Phys Conf Series 2009;180:012031.

[37] Clavin P. Dynamical behavior of premixed flame fronts in laminar and turbulent flows. Prog Energy Combust Sci 1985;11:1–59.

[38] Matalon M. Intrinsic flame instabilities in premixed and nonpremixed combustion. Annu Rev Fluid Mech 2007;39:163–91.

[39] Giannakopoulos GK, Gatzoulis A, Frouzakis CE, Matalon M, Tomboulides AG. Consistent definitions of "flame displacement speed" and "Markstein length" for premixed flame propagation. Combust Flame 2015;162:1249–64.

[40] Lipatnikov AN. Some issues of using Markstein number for modeling premixed turbulent combustion. Combust Sci Technol 1996;119:131–54.

[41] Bradley D, Gaskell PH, Gu XJ, Sedaghat A. Premixed flamelet modelling: factors influencing the turbulent heat release rate source term and the turbulent burning velocity. Combust Flame 2005;143:227–45.

[42] Karpov VP, Lipatnikov AN, Zimont VL. A test of an engineering model of premixed turbulent combustion. Proc Combust Inst 1996;26:249–57.

[43] Karpov VP, Severin ES. Effects of molecular-transport coefficients on the rate of turbulent combustion. Combust Explos Shock Waves 1980;16:41–6.

[44] Peters N. Turbulent combustion. Cambridge University Press; 2000.

[45] Poinsot T, Veynante D. Theoretical and numerical combustion. Edwards. 2nd ed. 2005.

[46] Bilger RW, Pope SB, Bray KNC, Driscoll JF. Paradigms in turbulent combustion research. Proc Combust Inst 2005;30:21–42.

[47] Chakraborty N, Champion M, Mura A, Swaminathan N. Scalar-dissipation-rate approach [Chapter 4]. In: Swaminathan N, Bray KNC, editors. Turbulent premixed flames. Cambridge University Press; 2011. p. 74–102.

[48] Karpov VP, Lipatnikov AN, Zimont VL. Flame curvature as a determinant of preferential diffusion effects in premixed turbulent combustion [chapter 14]. In: Sirignano WA, Merzhanov AG, de Luca L, editors. Advances in combustion science: in honor of ya.B. Zel'dovich. vol. 173. Prog Astronaut Aeronautics; 1996. p. 235–50.

[49] Lipatnikov AN, Chomiak J. Lewis number effects in premixed turbulent combustion and highly perturbed laminar flames. Combust Sci Technol 1998;137:277–98.

[50] Sabelnikov VA, Lipatnikov AN. Transition from pulled to pushed premixed turbulent flames due to countergradient transport. Combust Theor Model 2013;17:1154–75.

[51] Sabelnikov VA, Lipatnikov AN. Transition from pulled to pushed fronts in premixed turbulent combustion: theoretical and numerical study. Combust Flame 2015;162:2893–903.

[52] Kha KQN, Robin V, Mura A, Champion M. Implications of laminar flame finite thickness on the structure of turbulent premixed flames. J Fluid Mech 2016;787:116–47.

[53] Kim SH. Leading points and heat release effects in turbulent premixed flames. Proc Combust Inst 2017;36:2017–24.

[54] Dave HL, Mohan A, Chaudhuri S. Genesis and evolution of premixed flames in turbulence. Combust Flame 2018;196:386–99.

[55] Lipatnikov AN, Chakraborty N, Sabelnikov VA. Transport equations for reaction rate in laminar and turbulent premixed flames characterized by non-unity Lewis number. Int J Hydrogen Energy 2018;43(45):21060–9.

[56] Kee R, Miller J, Evans G, Dixon-Lewis G. A computational model of the structure and extinction of strained, opposed flow, premixed methane-air flames. Proc Combust Inst 1989;22:1479–94.

[57] Lutz AE, Kee RJ, Grcar JF, Rupley FM. OPPDIF: a Fortran program for computing opposed-flow diffusion flames. Sandia National Laboratories Report SAND96-8243; 1996.

[58] Kee RJ, Rupley FM, Miller JA. CHEMKIN-II: a FORTRAN chemical kinetics package for the analysis of gas-phase chemical kinetics. Sandia National Laboratories Report SAND89-8009, 1989.

[59] Davis SG, Joshi AV, Wang H, Egolfopoulos F. An optimized kinetic model of H_2/CO combustion. Proc Combust Inst 2005;30(1):1283–92.

[60] Goswami M, Bastiaans RJM, Konnov AA, de Goey LPH. Laminar burning velocity of lean H_2-CO mixtures at elevated pressure using the heat flux method. Int J Hydrogen Energy 2014;39:1485–98.

[61] Kéromnès A, Metcalfe WK, Heufer KA, Donohoe N, Das AK, Sung CJ, Herzler J, Naumann C, Griebel P, Mathieu O, Krejci MC, Petersen EL, Pitz WJ, Curran HJ. An experimental and detailed chemical kinetic modeling study of hydrogen and syngas mixture oxidation at elevated pressures. Combust Flame 2013;160:995–1011.

[62] Li J, Zhao Z, Kazakov A, Chaos M, Dryer FL, Scire Jr JJ. A comprehensive kinetic mechanism for CO, CH_2O, and CH_3OH combustion. Int J Chem Kinet 2007;39:109–36.

[63] Wu F, Liang W, Chen Z, Ju Y, Law CK. Uncertainty in stretch extrapolation of laminar flame speed from expanding spherical flames. Proc Combust Inst 2015;35:663–70.

[64] Marshall A, Venkateswaran P, Noble D, Seitzman J, Lieuwen T. Development and characterization of a variable turbulence generation system. Exp Fluid 2011;51:611–20.

[65] Lipatnikov AN, Chomiak J. Turbulent flame speed and thickness: phenomenology, evaluation, and application in multi-dimensional simulations. Prog Energy Combust Sci 2002;28(1):1–74.

[66] Yu R, Lipatnikov AN. Direct numerical simulation study of statistically stationary propagation of a reaction wave in homogeneous turbulence. Phys Rev E 2017;95:063101.

[67] Lipatnikov AN, In De S, Agarwal AK, Chaudhuri S, Sen S, editors. Modeling and simulation of turbulent combustion. Springer Nature Singapore Pte Ltd; 2018. p. 181–240.

[68] Zimont VL, Lipatnikov AN. To computations of the heat release rate in turbulent flames. Dokl Phys Chem 1993;332:592–4.

[69] Zimont VL, Lipatnikov AN. A numerical model of premixed turbulent combustion of gases. Chem Phys Reports 1995;14(7):993–1025.

[70] Yasari E, Verma S, Lipatnikov AN. RANS simulations of statistically stationary premixed turbulent combustion using Flame Speed Closure model. Flow, Turbul Combust 2015;94:381–414.

[71] Verma S, Lipatnikov AN. Does sensitivity of measured scaling exponents for turbulent burning velocity to flame configuration prove lack of generality of notion of turbulent burning velocity? Combust Flame 2016;173(1):77–88.

[72] Bray KNC, Moss JB. A unified statistical model of the premixed turbulent flame. Acta Astronaut 1977;4:291–319.

[73] Libby PA, Bray KNC. Variable density effects in premixed turbulent flames. AIAA J 1977;15:1186–93.

[74] Prudnikov AG, In Raushenbakh VB, editors. Physical principles of the working process in combustion chambers of jet engines. Clearing House for Federal Scientific & Technical Information; 1967. p. 244–336.

[75] Lipatnikov AN, Chomiak J. Self-similarly developing, premixed, turbulent flames: a theoretical study. Phys Fluids 2005;17:065105.

[76] Lipatnikov AN, Chomiak J. Developing premixed turbulent flames: Part I. A self-similar regime of flame propagation. Combust Sci Technol 2001;162:85–112.

[77] Driscoll J. Turbulent premixed combustion: flamelet structure and its effect on turbulent burning velocities. Prog Energy Combust Sci 2008;34:91–134.

[78] Kuznetsov VR. Certain peculiarities of movement of flame front in a turbulent flow of homogeneous fuel mixtures. Combust Explos Shock Waves 1975;11:487–93.

[79] Clavin P, Williams FA. Theory of premixed-flame propagation in large-scale turbulence. J Fluid Mech 1979;90:589–604.

[80] Zimont VL. Theory of turbulent combustion of a homogeneous fuel mixture at high Reynolds number. Combust Explos Shock Waves 1979;15:305–11.

[81] Zimont VL. Gas premixed combustion at high turbulence. Turbulent flame closure combustion model. Exp Therm Fluid Sci 2000;21:179–86.

[82] Karlovitz B, Denniston DW, Wells FE. Investigation of turbulent flames. J Chem Phys 1951;19:541–7.

[83] Lipatnikov AN, Chomiak J. A simple model of unsteady turbulent flame propagation. SAE Trans Sect 3, J Engines 1997;106:2441–52.

[84] Lipatnikov AN, Chomiak J. Transient and geometrical effects in expanding turbulent flames. Combust Sci Technol 2000;154:75–117.

[85] Lipatnikov AN. Can we characterize turbulence in premixed flames? Combust Flame 2009;156:1242–7.

[86] Lipatnikov AN, Chomiak J. Effects of premixed flames on turbulence and turbulent scalar transport. Prog Energy Combust Sci 2010;36(1):1–102.

[87] Sabelnikov VA, Lipatnikov AN. Recent advances in understanding of thermal expansion effects in premixed turbulent flames. Annu Rev Fluid Mech 2017;49:91–117.

[88] Pope SB. Ten questions concerning the large-eddy simulation of turbulent flows. New J Phys 2004;6:1–24.

[89] Launder BE, Spalding DB. Mathematical models of turbulence. London: Academic Press; 1972.

[90] El Tahry SH. k-epsilon equation for compressible reciprocating engine flows. J Energy 1983;7(4):345–53.

[91] Chomiak J, Nisbet J. Modeling variable density effects in turbulent flames - some basic considerations. Combust Flame 1995;102:371–86.

[92] Weller HG, Tabor G, Jasak H, Fureby C. A tensorial approach to computational continuum mechanics using object-oriented techniques. Comput Phys 1998;12(6):620–31.